Capabilities of a coupled 1D/2D model for flood inundation simulation

Antonin Maugeri

Engineering student, School for Water and Environmental Engineering (ENGEES), Columbia Water Center summer internship
24 July 2012

Abstract

In this paper, the functioning, capabilities and limitations of a physically-based flood inundation model are discussed. Channel flow is represented by a kinematic one dimensional wave procedure through cross sections which is solved numerically by a finite difference scheme and floodplain routing is a two dimensional procedure that allows water to flow from cell to cell over a raster grid. A French area, concerned by flood problems, is modeled and the data requirement is exposed in this order : Digital Elevation Model, inflow discharge hydrographs and channel components. The creation of input hydrographs used for simulations is detailed. Using simulation results, the effects of time step and grid scale parameters on computational time and model accuracy is firstly exposed. The roughness sensitivity is then evaluated by testing effects of the Manning's friction coefficient for channel and floodplain on simulated flood extent and bulk characteristics. We thus establish that model is insensitive to floodplain roughness but highly sensitive to channel roughness. It allows us to compete a calibration and validation procedure for the modeled area. Starting from obtained results and previous publications several points are discussed : computational efficiency, roughness sensitivity, calibration and validation assessment and best scale modeling. We conclude that the studied model, thanks to its smart coupled 1D/2D procedure, is computationally efficient. Moreover, it is able to compete calibration and validation process trough the channel roughness, despite its unintuitive behavior for floodplain roughness. The model is best suited for middle-sized rural area (typically 10 km reaches), and could be adapted to large scale area by adding runoff/rainfall components but is not designed for urban simulations because of its over simplification which is however an advantage for the other uses.

1. Introduction

Flood modeling is an important task for decision making in the field of natural risk management. Therefore river engineers and managers need designed tools, as physically-based models, in order to evaluate flood inundation risk. The goal of such tools is to simulate probable inundation damage on a given area depending on several flood scenarios with different intensity, duration and return period. Model reliability is assessed by confronting simulation results and real data in a calibration process : starting from a real inundation that occurred, with a given return period, difference between real data and output modeled data is minimized by adjusting some parameters of the model. Starting from these adjusted parameters, the model is then validated by checking that difference is acceptable for other flood events with available real data. But such model assessment method is not straightforward at all. Research in this field concerns model development, through physical equations used and simplification level, and confidence level assessment a the calibration/validation step, that is to say methodology of comparison between real data and simulations.

In this paper, we study the case of the physically-based model LISFLOOD-FP developed by researchers at the University of Bristol (Bates and De Roo, 2000). Using the case of flood events at the scale of a French watershed we evaluate capabilities of this model that offers an original coupled 1D/2D approach, and also to carry on a larger reflection about flood modeling that can benefit to other kind of models.

Firstly, we present LISFLOOD-FP basis (physical principles and equations), then data requirement is exposed through the presentation of the area modeled and the inputs used (data set and building method). Secondly, we analysis model functioning by exposing simulation results (computational time, sensitivity to calibration parameters) and then we use these results in order to complete model assessment (calibration/validation process). Lastly, capabilities and limitations of the model are discussed and a conclusion about issues raised is drawn.

2. Model and data

2.1. Channel flow equations

As explained by its developers (Bates and De Roo, 2000), the first version of the LISFLOOD-FP model consists of a classical one dimensional hydraulic routine procedure through cross sections for channel flow. A simplification of the full one-dimensional St. Venant two-equation system, continuity (Eq. 1) and momentum (Eq. 2), leads to a kinematic wave approximation (by removing local acceleration, convective acceleration and pressure terms in the momentum equation). Note that developers have chosen Manning equation for the momentum equation (Eq. 2) among other alternative uniform flow formulae :

$$\frac{\partial Q}{\partial x} + \frac{\partial A}{\partial t} = 0 \quad \text{(Eq. 1)}$$

$$\mathrm{S}_0 = \frac{n^2 P^{4/3} Q^2}{A^{10/3}} \quad \text{(Eq. 2)}$$

Q is the volumetric flow rate in the channel, A the cross sectional of the flow, S_0 the slope of the bed, n the Manning's coefficient of friction (contribution of this parameter will be discussed in Section V.), and P the wetted perimeter of the flow. An important assumption is that the channel is wide and shallow so the wetted perimeter is approximated by the channel width.

Expect for a few special simple cases this system does not have analytical solutions and leads to numerical methods as finite difference approximation (Chow, 1988). Streamflow and cross section values are calculated with a simple linear scheme that uses a backward-difference method to derive the finite difference equations. Eq. 1 and Eq. 2 are combined to obtain the following equation :

$$\frac{\partial Q}{\partial x} + \frac{3}{5}\alpha Q^{-2/5}\frac{\partial Q}{\partial t} = 0 \quad \text{(Eq. 3)}$$

with the constant value

$$\alpha = \frac{n^{3/5} b^{2/5}}{S_0^{3/10}} \quad \text{(Eq. 4)}$$

where b is the channel width.

The finite difference equation can be set up in order to calculate the quantity Q_i^j at each node (i, j), where i represents the space and j the time :

$$\frac{\partial Q}{\partial x} = \frac{Q_{i+1}^{j+1} - Q_i^{j+1}}{\Delta x} \quad \text{(Eq. 5)}$$

$$\frac{\partial Q}{\partial t} = \frac{Q_{i+1}^{j+1} - Q_{i+1}^{j}}{\Delta t} \quad \text{(Eq. 6)}$$

in order to create a linear equation, the value of Q in the expression $\frac{3}{5}\alpha Q^{-2/5}$ of (Eq. 3) is found by averaging the following values :

$$Q = \frac{Q_i^{j+1} + Q_{i+1}^{j}}{2} \quad \text{(Eq. 7)}$$

As boundary condition, an imposed flow at the upstream end of the reach provides the value for i=0 for each time step j. Similarly, as initial conditions pairs (i, j=0) are known for each space step i. By substitution of Eq. 5, Eq. 6 and Eq. 7 in Eq. 3 the value of Q_{i+1}^{j+1} can be calculated knowing Q_i^j, Q_{i+1}^j and Q_i^{j+1} (Fig. 1 and Eq. 8). Cross section A_i^j can be calculated at each node using (Eq. 2). Finally, thanks to the assumption of a rectangular channel, water depth is obtained at each section, at each time step (with $h_i^j = A_i^j / b_i^j$). For a given channel cell, once the bankful depth is exceeded, water can be routed into adjacent floodplain areas of the raster grid

$$Q_{i+1}^{j+1} = \frac{\frac{\Delta t}{\Delta x} Q_i^{j+1} + \frac{3}{5}\alpha Q_{i+1}^j \left(\frac{Q_i^{j+1}+Q_{i+1}^j}{2}\right)^{-2/5}}{\frac{\Delta t}{\Delta x} + \frac{3}{5}\alpha \left(\frac{Q_i^{j+1}+Q_{i+1}^j}{2}\right)^{-2/5}} (Eq.8)$$

Fig. 1. Finite difference box for the linear kinematic wave equation

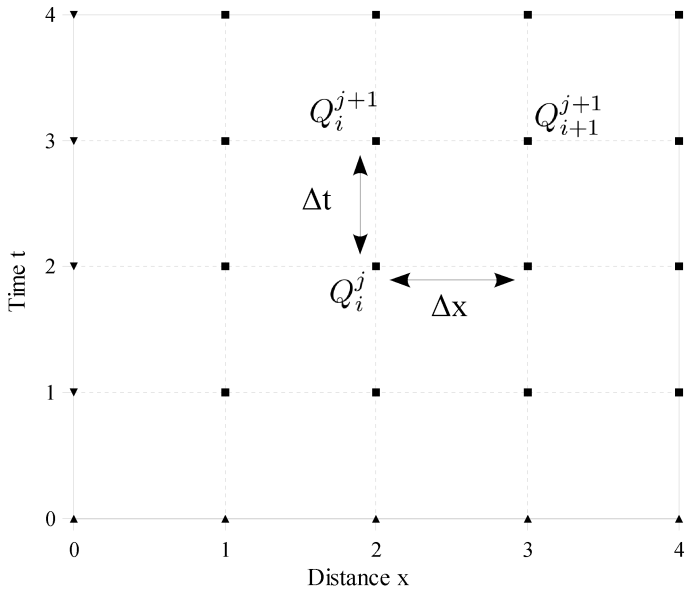

2.2. Floodplain flow equations

Floodplain flows in LISFLOOD-FP are described with classical continuity and momentum equations, discretized over a grid of square cell (as described in Section 2.3. (i)) wich allows for the representation of the two-dimensional dynamic flow on the flood plain. Starting from a simple continuity equation for a given cell :

$$\frac{dV}{dt} = Q_{up} + Q_{down} + Q_{left} + Q_{right} \qquad \text{(Eq. 9)}$$

where dV is the volume variation during time dt, Q_{up}, Q_{down}, Q_{left} and Q_{right} are the volumetric flow rate repectively coming from the up, the down, the left and the right adjacent cells of the grid. Flow between two cells is assumed to be simply a function of the free surface height difference between these cells, hence the following discretisation of continuity Eq. 1 (Fig. 2, Eq. 10 and Eq. 11) :

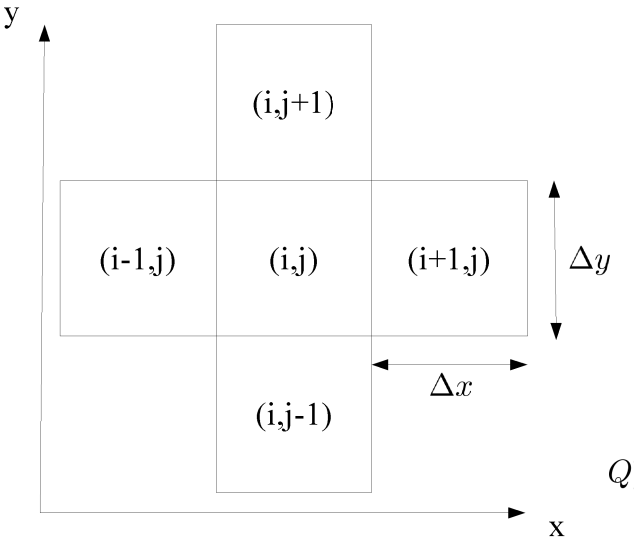

Fig. 2. Discretization scheme for floodplain grid

$$\frac{dh^{i,j}}{dt} = \frac{Q_x^{i-1,j} + Q_x^{i,j} + Q_y^{i,j-1} + Q_y^{i,j}}{\Delta x \Delta y} \text{ (Eq. 10)}$$

where h_i^j is the water free surface height at the node (i,j), Δx and Δy are the cell dimensions, n is the Manning's friction coefficient for the flood plain, Q_x and Q_y represent the volumetric flow rates between floodplain cells and are defined by the following momentum equation :

$$Q_x^{i,j} = \pm \frac{h_{flow}^{5/3}}{n} \left(\frac{|h^{i+1,j} - h^{i,j}|}{\Delta x} \right)^{1/2} \Delta y \quad \text{(Eq. 11)}$$

where h_{flow} represents the depth through wich water can flow between two cells, and is defined as the diffrence between the highest water free surface in the two cells and the highest bed elevation (according to developers this definition has been found to give reasonable results). Note that the momentum equation (Eq. 11) for Q_x, Q_y, similarly to channel flow (Eq. 2), corresponds to the Manning equation.

Fig. 3. Floodplain flow between two cells (Eq. 11)

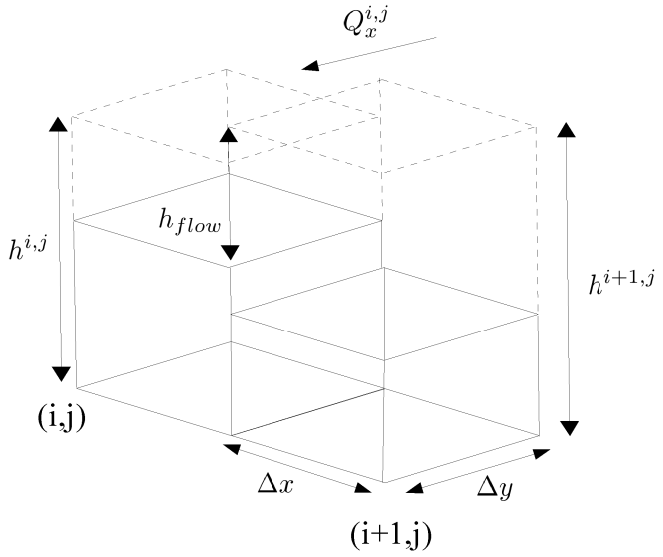

2.3. Area modeled

In order to evaluate the LISFLOOD-FP capabilities a catchment area concerned about flood inundation has been modeled. The corresponding watershed (724 km2) is located in Brittany in the west of France. Its main river is the Odet (62 km) whose two main tributary rivers are the Jet (28,5 km) and the Steïr (27,0 km). The area has known several flood events at the confluence of three main rivers where the city of Quimper is located (approximately 60.000 inhabitants). Indeed, according to the archives of this city several flood events occurred in the past (1651, 1664, August 1769, 1788, February 1838, March 1846, June 1856, December 1865, February 1883, November 1892, January 1925, January 1928, February 1935, April 1939, 1957 and February 1974). More recently, two major events in Brittany, in January 1995 and December 2000-January 2001 (respectively of 50 and close to 100 years return period), led to major effects on goods and people. Fig. 4 below represents the area modeled at different scales :

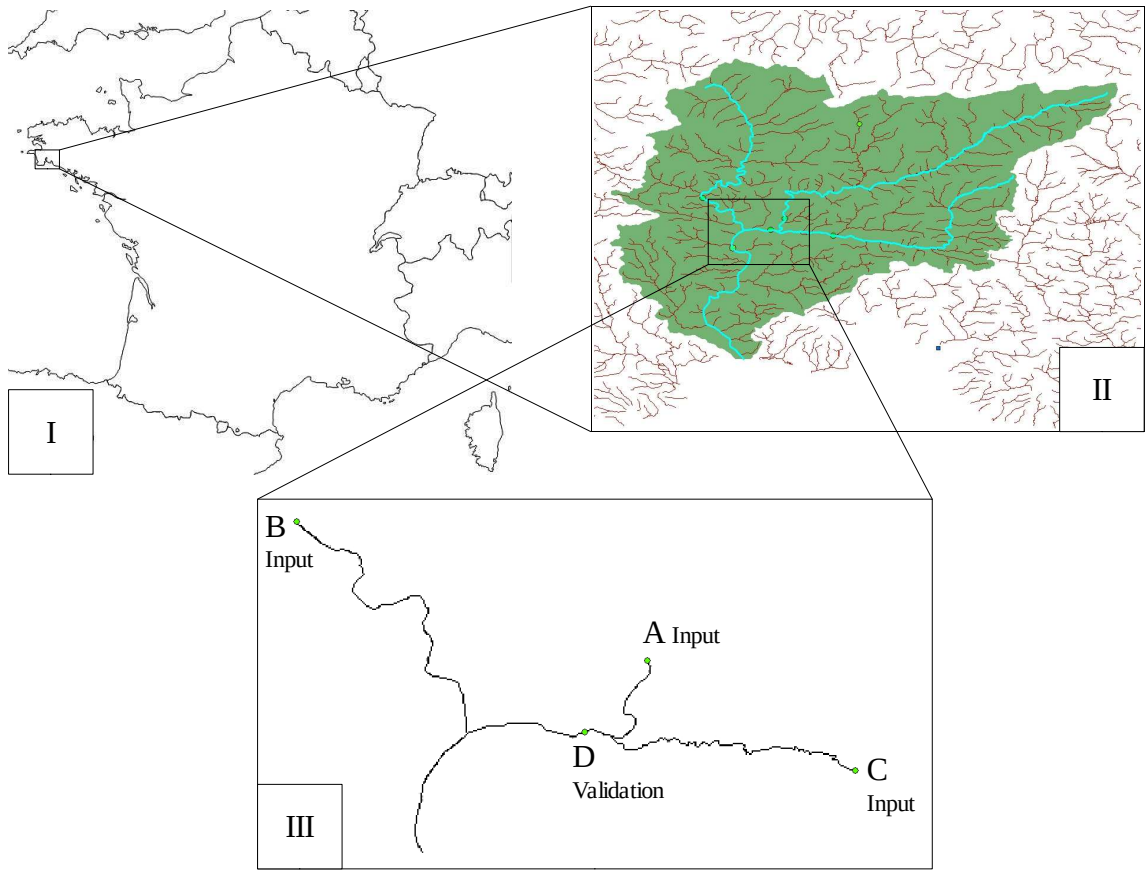

Fig. 4. Area modeled. Top left : watershed modeled at the French scale (II). Top right : river network in the delimited watershed (II). Below (III), network model with inputs node A, the Odet at Ergué-Gabéric, node B, the Steïr at Guengat, node C, the Jet at Ergué Gaberic and validation node D, the Odet at Quimper.

The data requirement of LISFLOOD-FP can be summarized as follows ; (i) Digital elevation model (DEM) raster grid, (ii) inflow discharge hydrographs and (iii) channel components.

(i) The DEM raster grid allows the representation of a complex flood plain topography and is linked with current improvement of remote sensing technologies. Indeed, it is an increasing of DEM data availability obtained by air photogrammetry, airborne laser altimetry (LiDAR) and interferometric Synthetic Aperture Radar (SAR). Note that such technologies are able to product data set in raster format directly usable on GIS software (ArcGIS, MapInfo) and often free to access. In this study, raster grid used comes from data acquired by a NASA satellite sensor ASTER : Global Digital Model Elevation data set (ASTER GDEM) and freely accessible on the relative website (www.gdem.aster.ersdac.or.jp).

(ii) For the discharge hydrographs, the French data set *Banque Hydro* has been used

(www.hydro.eaufrance.fr). It contains 3.500 gauging stations that measure daily streamflows for the entire French river network. For the study-concerned watershed, three gauging stations (A, B, C of Fig. 4) are used in order to create input hydrographs for boundary conditions of the model (as explained further in Section 2.4.) and an additional station (D of Fig. 4), internal to the domain, is used as validation data. It offers an horizontal accuracy of 25m. The area modeled is composed of approximately 90k cells.

(iii) For the channel components, the river layout has been geolocated using the GIS data set *BD Carthage* that includes both main rivers and tributaries. River width has been obtained with web GIS that offers high precision distance measuring by satellite imagery (Google Earth) and direct mapping (GIS of Quimper, sig-diffusion.quimper-communaute.fr). In order to obtain the most realistic model, down slope and bankful depth have been filled from topography and known elevation at each measurement station.

Some minor tributaries were not represented in the model for two reasons. Firstly, there is a lack of data concerning these reaches (hydraulic data for inflow discharge hydrographs and channel components information). Secondly, the runoff contributing area which is concerned by input nodes A, B, C was calculated and represents a surface area of 68% compare to the whole watershed studied. So it was considered that hydrological contribution of minor tributaries not represented not the model is negligible.

The whole data are firstly imported in GIS software ArcMap, secondly projected in the same geodetic system (WGS 84), thirdly reprojected in a single Cartesian coordinates frame (UTM Zone 30 N) and finally exported as text files workable by the LISFLOOD-FP software. Note that the initial conditions have to be obtained by stabilization of a preliminary steady state simulation before running the dynamic simulations.

2.4. Hydrographs creation

Input hydrographs at the nodes A, B and C of Fig. 4 have been created using streamflow data described in the Section 2.3. (ii). The record event, both in term of water depth and instantaneous stream flow, has been selected from this data set in order to create input hydrographs of the model. For each gauging station, record event occurred in 2001 in the night of December 12th to 13th and led to significant flood damage. Selected daily hydrographs range from December 1st to 25th : this duration is sufficient to correctly represent day by day the event. However, the model requires hourly inputs hydrographs which means a conversion from values of 25 days to 600 hours. Starting from these daily measured hydrographs, a piecewise linear function was created in order to obtain hourly input hydrographs as shown in Fig. 5 (example of node A). Moreover, measured instantaneous peaks have been included in the input hydrographs thereby created. Obviously, each instantaneous peak exceeds the corresponding mean daily value creating therefore an overestimation of volume for the input hydrograph created compare to the measured hydrograph.

Fig. 5. Hourly stream flow input of the model for the node A (grey line) built from daily streamflow at the corresponding measurement station (black line). Here is represented the exemple of the node A, the Odet at Ergué-Gabéric. Other input nodes (B and C) have been defined following the same method.

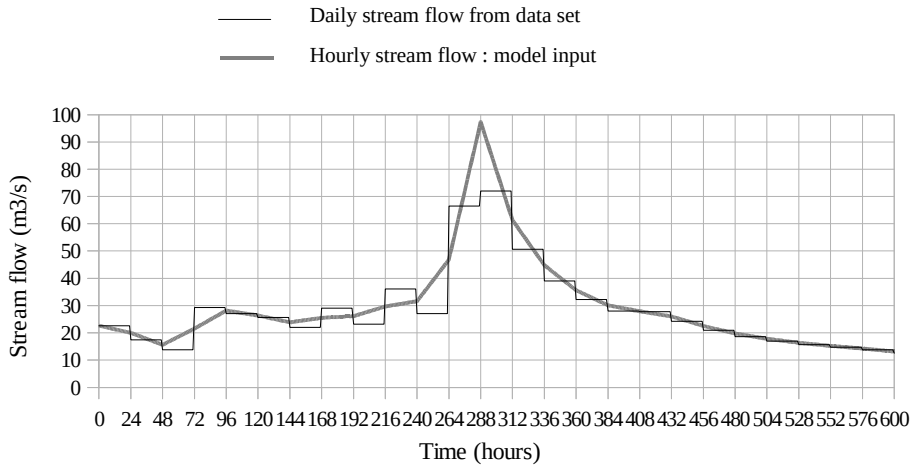

However, resulting overestimation of volume is acceptable (Table 1).

Table 1. Calculated flood volume for the 2001 event (FloodVol) from measured daily streamflow data and overestimated percentage for the volume (InputVol) of hourly input hydrograph corresponding where : **Input overestimation = (InputVol ─ FloodVol)/FloodVol**

Node	FloodVol : measured flood volume (10^6 m^3)	Input overestimation (%)
A the Odet at Ergué-Gabéric	62,77	2,20%
B the Steïr at Guengat	49,10	5,63%
C the Jet at Ergué-Gabéric	25,71	3,97%

3. Results

3.1. Time step and grid scale

Starting from the original 25m resolution, three other raster grids (50m, 75m, 100m) have been created by aggregating mean values. For each of these DEM grids, different fixed time steps (1s, 5s, 10s, 100s, 1000s) have been tested in order to evaluate computational times. Manning's friction coefficients are those initially filled in the model (model sensitivity to these important hydraulic parameters is studied in the next parts). Results of computational times (in min) obtained are shown in Table 2 below :

Table 2. Computational times (in min) depending on grid size and time step.

	1s	5s	10s	100s	1000s
25 m	51	42	20	2	2
50 m	51	10	5	2	1
75 m	25	5	2	1	1
100 m	18	4	2	2	1

The next step is to evaluate effect on model accuracy depending on changes of fixed time step and space resolution. Intuitively we can expect that the more precise the parameters are (a low time step and a high space resolution) the more reliable results will be. A former study (Bates and De Roo, 2001b) has shown that the increasing of model space resolution does not necessarily improves accuracy of simulations. However, in our case, hydrographs at the validation point are poorly fitting with measured streamflows when space resolution decreases for a fixed time step (Fig.6).

Fig. 6. Simulated hydrographs depending on grid resolution compared to measured hydrograph at the validation point D (the Odet et Quimper). Time step is Δt = 1s.

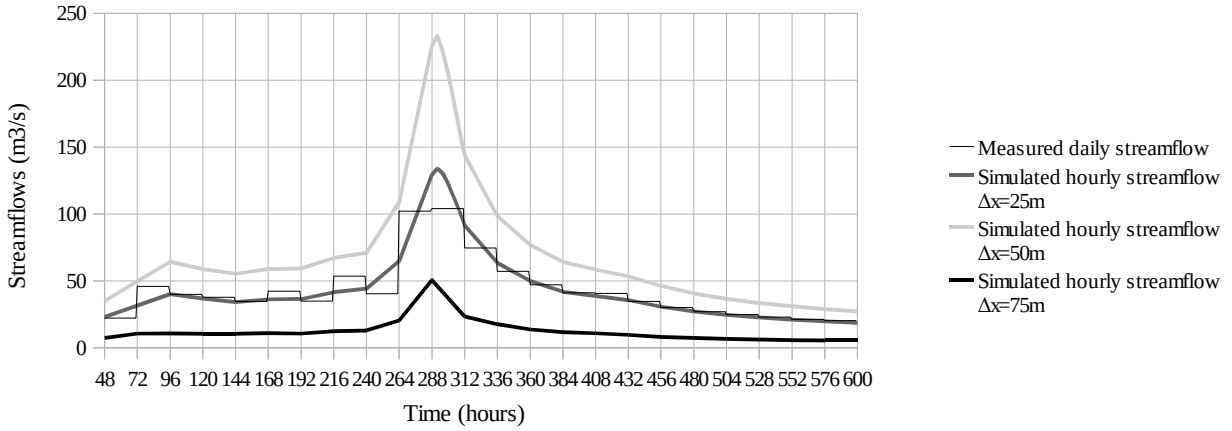

Another time parameter was tested, the Adaptive Time Stepping (ATS), which is an algorithm implemented in the code and that allows it to calculate adapting time values at each computational step. The main

advantage of the ATS (as shown by Hunter et al., 2005) is to yield results that were independent of grid size or choice of initial time step and which showed an intuitively correct sensitivity to floodplain friction. However, these improvements were obtained with simplified models. A problem with this approach is that there is no lower bound on the time step. Indeed, for this reason, simulations for the 25 m grid resolution in our case can not been obtained. Moreover, simulation times with the ATS become not negligible, especially when Manning's floodplain friction n_{fp} coefficient becomes small (Table 3).

Table 3. Computational time with Adaptive Time Stepping (ATS) depending on floodplain roughness n_{fp} (friction coefficient for channel n_{ch} is equal to 0.03).

	ATS (n_{fp}=0.20)	ATS (n_{fp}=0.06)	ATS (n_{fp}=0.01)
25 m	Can not be completed	Can not be completed	Can not be completed
50 m	1h30	4h30	**More than 24h**

3.2. Model's sensitivity to Manning's friction coefficients

3.2.1 Generalities about Manning's parameters

Manning's friction coefficient n ($m^{-1/3}.s^{-1}$), or its reciprocal the Strickler coefficient K=1/n, is a parameter that characterizes flow resistance or “roughness” for both the channel and floodplain flow equations (Section 2). According to Chow (1959) Manning's main channel friction coefficient varies from 0,03 (clean, straight, full stage, no rifts or deep pools) to 0,1 (very weedy reaches, deep pools, or flood ways with heavy stand or timber and underbrush) and Manning's floodplain friction coefficient from 0,03 (pasture with no brush and short grass) to 0,120 (heavy stand of timber, a few down trees, little undergrowth, flood stage below branches with flood stage below branches). According to LISFLOOD-FP's developers (Bates and De Roo, 2000), as with all hydraulic models, sensitivity to friction factor values is to be expected in dynamic simulations and examination of model response to the friction parameter variation should be a part of any further study.

3.2.2. Inundation extent sensitivity to Manning's coefficient

The goal of the first set of simulations was to test the sensitivity of the model to different values of a spatially uniform Manning's floodplain friction coefficient. For each simulation, the value of Manning's channel friction coefficient is set constant and equal to the original parameter as defined in the model (i.e. n_{ch}=0,03). The model's sensitivity is evaluated with the number of pixels inundated during the maximum flood extent (.MAX). Raster DEM and channel components are those exposed in Section 2.3. As well, input hydrographs at nodes A, B and C are those described in Section 2.4. A fixed time step is considered here (Δt=10s). Results of simulations (Table 4), even for interval that includes largely unrealistic values, show clearly that the model is insensitive to Manning's floodplain friction coefficient.

Simulation i	i=1	i=2	i=3	i=4	i=5	i=6
Manning's n_{ch}	0,03	0,03	0,03	0,03	0,03	0,03
Manning's n_{fp}	10	1	0,1	0,06	0,01	0,001
WaterPix(i)	1953	2049	2098	2099	2100	2100
S(%)	-6,956%	-2,382%	-0,048%	0,000%	0,048%	0,048%

Table 4. Flood extent sensitivity S(%) to Manning's floodplain friction coefficient. For each simulation, flood extent is compared to the flood extent for the original friction parameter pair of the model (n_{ch}=0,03 ; n_{fp}=0,06) as follow :

$$S(\%) = (WaterPix(i)-WaterPixOp)/WaterPixOp,$$

where ;
WaterPix(i) = Number of water pixels for the given simulation i (n_{ch}=0,03 ; n_{fp}*(i)*);
WaterPixOp = Number of water pixels for the simulation with the original pair (n_{ch}=0,03 ; n_{fp}=0,06).

The same method has been applied in order to test the sensitivity of the model to different values of a spatially constant Manning's channel friction coefficient. In this case, value of Manning's floodplain friction coefficient is set spatially uniform and equal to the original parameter as defined in the model (i.e. n_{fp}=0,06).Contrary to previous results, simulations show clearly that the model is highly sensitive to Manning's channel friction coefficient (Fig. 7, simulation 7 to 16). A linear trend between model sensitivity and Manning's channel friction coefficient appears clearly on the graph.

Fig. 7. Model sensitivity S(%) to Manning's channel friction coefficient. Simulation i=7 to 16.

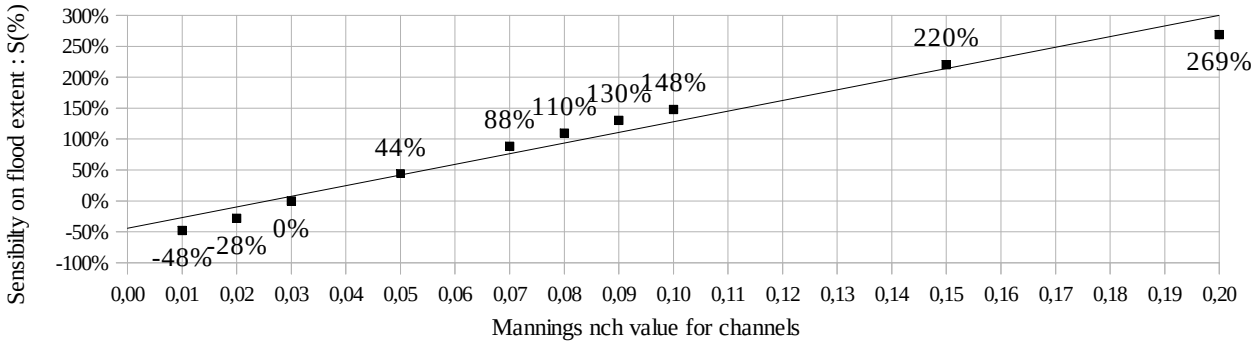

Δx= 25m, Δt=10s , Manning's flood plain nfp=0,06

Equation of the linear trend (continuous line) : y = 17,23x - 0,44

3.2.3. Bulk flood characteristics sensitivity to Manning's coefficients

Another way to evaluate the model's sensitivity to the friction coefficients is through the bulk flood characteristics which are wave volume, peak value and travel time. For each simulation (1 to 16) modeled output hydrographs at the node validation D have been extracted in order to compare model responses. The data set (described in Section W) allows us to compare simulated volume to measured volume at this node. When flood plain friction coefficient is the variable parameter (simulations 1 to 6) no model sensitivity has been noted similarly to results concerning inundation extent (Table 4). Contrary, as shown in Fig. 9, a model's variability depending on Manning's channel friction values is found.

Fig. 9. Simulated hydrographs (at node D) depending on Manning's channel friction coefficient

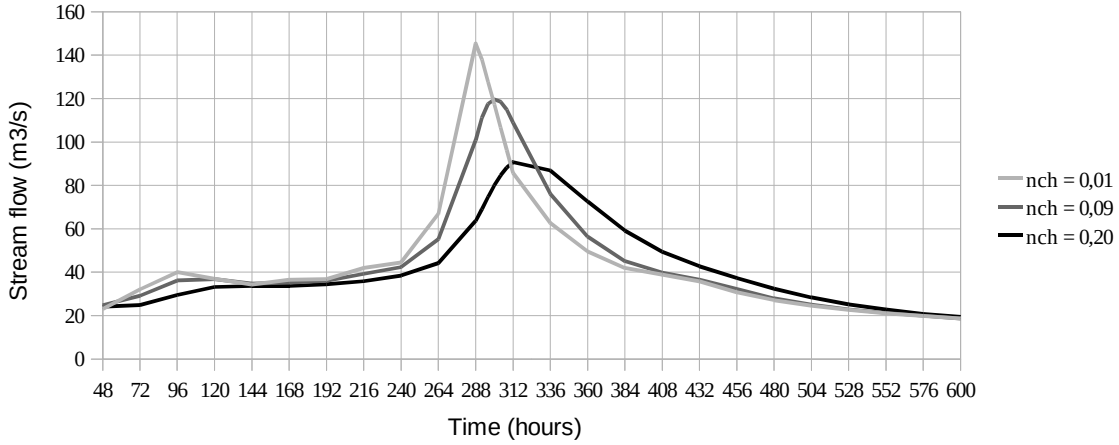

Δt =10s, Manning's flood plain nfp=0,06

Fig. 10 shows the evolution of total flood volume modeled depending on Manning's channel value. Polynomial interpolation (by Lagrange polynomials for instance) seems satisfactorily to establish a direct mathematical relation between Manning's channel friction and flood volume at the output point.

Fig. 10. Simulated flood volume (10^6 m^3) depending on Manning's channel friction coefficient (points)

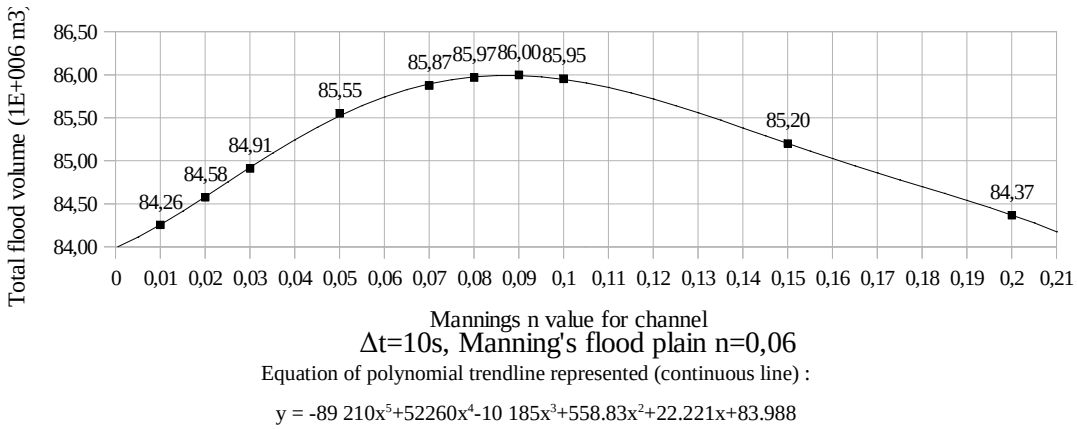

Equation of polynomial trendline represented (continuous line) :

$y = -89\,210x^5+52260x^4-10\,185x^3+558.83x^2+22.221x+83.988$

Concerning maximum values of modeled hydrographs, simulations show a linear relation between peak response and Manning's channel friction coefficient (Fig. 11).

Fig. 11. Simulated peak values (at point D) depending on Manning's channel friction coefficient

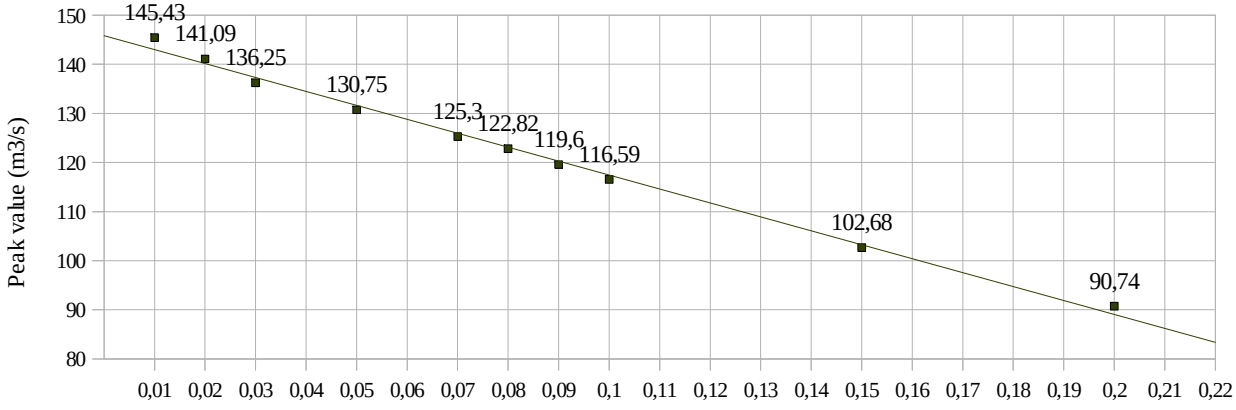

Equation of the linear trend (continuous line) : y = -283,94x+145,84

3.3 Calibration and validation

With available data concerning flood volume and peak a calibration was completed with the flood event of December-January 2001 (Section 2.3 and 2.4). As shown in Table 5, satisfactory accuracy is achieved. However, the optimum calibrations, for peaks or volume, are reached with different pairs of Manning's parameters.

Table 5. Calibration process based on comparison between measured data and simulated results of flood volume and maximum peak.

n_{fp}	0,06	0,06	0,06	0,06	0,06	0,06	0,06	0,06	0,06	0,06
n_{ch}	0,01	0,02	0,03	0,05	0,07	0,08	0,09	0,1	0,15	0,2
Simulated volume (m3/s)	84,26	84,58	84,91	85,55	85,87	85,97	86	85,95	85,2	84,37
Measured volume $(10^6 m^3)$	86,31	86,31	86,31	86,31	86,31	86,31	86,31	86,31	86,31	86,31
Error on volumes	-2,38%	-2,01%	-1,62%	-0,88%	-0,51%	-0,40%	**-0,37%**	-0,42%	-1,29%	-2,25%
Simulated peak (m3/s)	145,43	141,09	136,25	130,75	125,3	122,82	119,6	116,59	102,68	90,74
Measured peak (m3/s)	164	164	164	164	164	164	164	164	164	164
Error on peaks	**-11,32%**	-13,97%	-16,92%	-20,28%	-23,60%	-25,11%	-27,07%	-28,91%	-37,39%	-44,67%

The validation step was also completed using the flood event that occurred in January 1995. A lack of data concerning instantaneous peak at the validation node D constrained to establish validation step only with volume comparison. Manning's friction values are these determined by minimization of error on volume at the previous calibration step (n_{ch}=0,09, n_{fp}=0,06). Corresponding hydrographs are shown below (Fig. 10). The error on volume is 5,75%, so we can consider our model as validated for the flood volume parameter.

Fig. 10. Comparison of hydrograph simulated and measured at the validation step

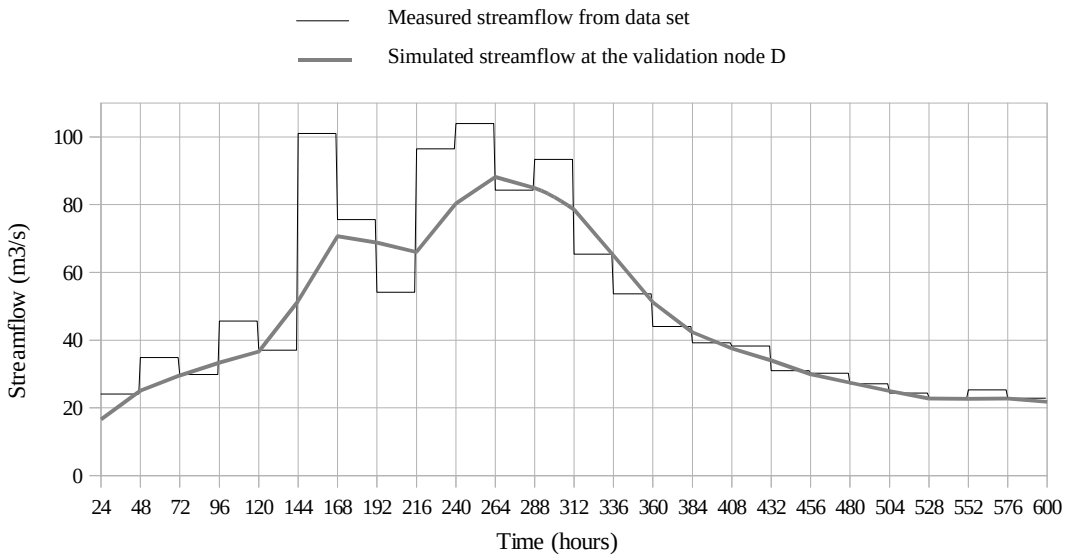

4. Discussion and conclusion

4.1. Discussion

Concerning computational costs, simulations have shown that LISFLOOD-FP responds to the assertion of its developers concerning a computational efficiency for fixed time steps even for a long duration simulation (25 days) over a large and complex topography. As we could expect, these computational costs are reduced with a larger time step and raster grid size (decreasing of space resolution). Despite of these improvements in computational times the maintaining of accuracy has to be insured depending of simulated results expected (inundation extent, water level or flood volume) in order to select the best compromise between low computational cost and maximum performance. Concerning the ATS option of the program we can see that computational costs become not negligible. Moreover, model sensitivity to floodplain friction coefficient (which was one of the purposes of the ATS development) was not observed for our studied case whereas changes in this parameter highly influences computational costs (from 1h30 to more than 24h). In addition, decreasing of grid size below 50m with the ATS option leads to infinite computational times.

Concerning roughness parameters, the model does not show an intuitive behavior concerning Manning's friction coefficient for floodplain. However, the high sensitivity to Manning's parameter for channels allows calibration by comparing simulated water level, simulated flood extent or simulated bulk with available data for a real event. One of the best advantage of the model, that we unfortunately could not use in our study because of a lack of data, is the direct comparison on GIS between simulated and measured flood extent (by using data imagery for a flood event). Indeed, whereas other calibration processes use to compare indirect simulated and measured parameters (as water depth for isolated points) this method presents the advantage to characterize directly the fit between model and reality with the flood extent, which is often the most important forecast required for flood risk management. However, the calibration and validation method proposed in our study leads us to the same conclusion as previous studies (Hunter and Bates, 2006, Horritt and Bates, 2001b) : while the model is capable of reproducing adequately either data set independently (in our case the flood volumes and the flood peaks), the optimal calibrations occur in different parts of the parameter space (two different pairs of Manning's friction coefficients). For a more precise calibration, especially in the case where it would be based on the flood extent, an idea is to divide channels with different Manning's values for each reach.

Finally, model improvement for further developments can be outlined. Whilst the LISFLOOD-FP seems, as shown in previous papers, a good tool for flood forecasting of rural areas (reaches from 3 km to 60 km), coastal areas (defense overtopping and defense breach for domain size from 100 to 1000 km^2) and even large-scale watersheds (Amazonian flooded wetlands, study of Wilson and Bates, 2007) some remarks may be expressed. On the one hand, the lack of rainfall/runoff components does not allows us to consider the purely hydrological effects and to benefit from the data availability concerning this aspect, especially for the research field. In the other hand, over simplification, in particular concerning channel components, is an obstacle to modeling urban areas whereflood risk is precisely the most important issue given the presence of lives and goods to protect.

4.2. Conclusion

LISFLOOD-FP model provides an efficient approach to flood modeling by selecting the advantages of both 1D and 2D flood models. The one-dimensional well-known routing procedure for channel flow allows an appropriate level of representation and a computational efficiency. While the original two-dimensional procedure allows the representation of floodplain flow over a complex topography by benefiting from increasingly accessible DEM data derived from remote sensing technologies. Thanks to the area modeled in this study, it has been confirmed that LISFLOOD-FP presents a lack of sensitivity to floodplain roughness which is the usual parameter of calibration in flood modeling. Despite this unintuitive behavior, the calibration and validation process can be successfully completed through the channel roughness. Capabilities of flood forecasting for rural medium-sized (typically reaches of 10 km long) and coastal areas is established

but serious large-scale modeling seems compromised without rainfall/runoff components. Lastly, concerning urban area modeling, its low level of complexity (which is an advantage on many other regards) does not allow LISFLOOD-FP, at this stage of development, to compete with other flood models specially dedicated to this task. However, the very interesting idea of such 1D/2D coupling principle seems to be applicable in such cases, the low level and the large scale, and may be the subject of further studies.

Acknowledgments

I would like to thank all the people at the Columbia Water Center for their kindest welcome and especially its director, Upmanu Lall, without whom I would not have got this internship and Tara Troy for her wise advices about publication writing and her support in rereading my work.

References

Hunter, N.M., Bates, P.D., Horritt, M.S. and Wilson, M.D. (2007). Simple spatially-distributed models for predicting flood inundation : a review. Geomorphology, 90, 208-225.

Wilson, M.D., Bates, P.D., Alsdorf, D., Forsberg, B., Horritt, M., Melack, J., Frappart, F. and Famiglietti, J. (2007). Modeling large-scale inundation of Amazonian seasonally flooded wetlands. *Geophysical Research Letters*, 34, paper no. L15404.

Hunter, N.M., Bates, P.D., Horritt, M.S. and Wilson, M.D., (2006). Improved simulation of flood flows using storage cell models. *Proceedings of the Institution of Civil Engineers, Water Management*, 159 (1), 9-18.

Hunter, N.M., Horritt, M.S., Bates, P.D., Wilson, M.D. and Werner, M.G.F., (2005). An adaptive time step solution for raster-based storage cell modelling of floodplain inundation. *Advances in Water Resources*, **28**, 975-991.

Horritt, M.S. and Bates, P.D., (2001b). Effects of spatial resolution on a raster based model of flood flow. *Journal of Hydrology*, **253**, 239-249.

Bates, P.D., De Roo, A.P.J., (2000). A simple raster-based model for floodplain inundation. *Journal of Hydrology*, **236**, 54-77.

Chow, V.T., Maidment, D.R., Mays, L.W., (1988). Applied hydrology, Mc-Graw Hill, New York (572 pp.).